

# Modeling the Temperature Fields of Copper Powder Melting in the Process of Selective Laser Melting

A A Saprykin<sup>1</sup>, E A Ibragimov<sup>1</sup>, E V Babakova<sup>1</sup>

<sup>1</sup>Yurga Institute of Technology, TPU Affiliate

E-mail: [Ibragimov@tpu.ru](mailto:Ibragimov@tpu.ru)

**Abstract:** Various process variables influence on the quality of the end product when SLM (Selective Laser Melting) synthesizing items of powder materials. The authors of the paper suggest using the model of distributing the temperature fields when forming single tracks and layers of copper powder PMS-1. Relying on the results of modeling it is proposed to reduce melting of powder particles out of the scanning area.

## 1. Introduction

A lot of process variables are taken into account when SLM synthesizing products. More than a hundred of variables are outlined in the literature, influencing somehow the SLM process [12], however, the researchers point at some key variables, inter alia: scanning speed; laser emission power; diameter of the laser; thickness of the powder layer; gaseous medium; the strategy of scanning. For instance, the authors [2–4, 8] have considered in details the relevance of speed of scanning, laser emission power, and powder thickness for synthesizing products of copper powder PMS-1. In papers [5–7] the impact of a gaseous medium on forming the single layers of copper powder is studied, as well as the effect of laser beam diameter on the thickness of the layer to be sintered is examined. The papers [9, 10] are focused on the importance of laser beam scanning strategy for development of thermal stresses and strains of the sintered samples.

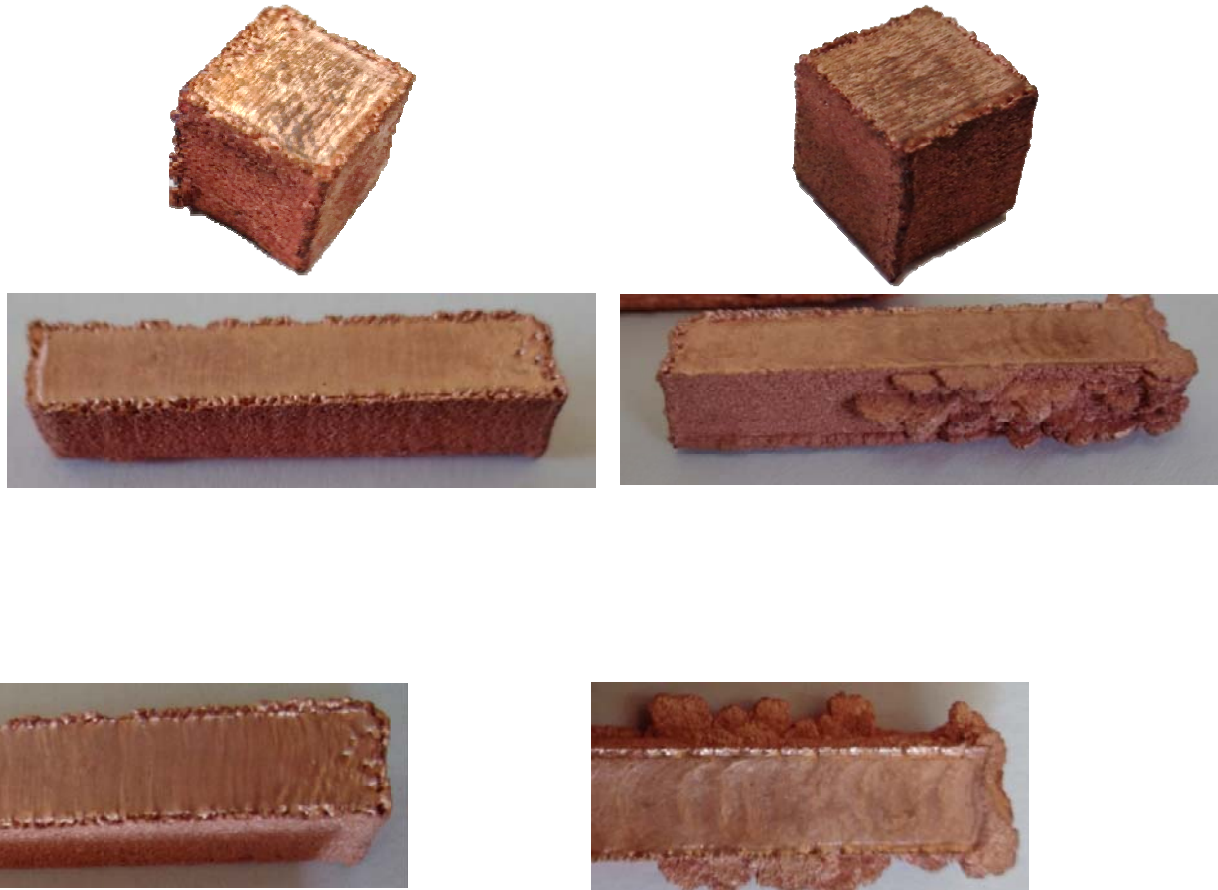
The most appropriate process conditions for sintering products of copper powder PMS-1 are determined on the base of research results outlined in paper [2]. Cubic samples with the sides 10×10×10 mm (Figure 1) are produced in these conditions. The mechanical compressive strength of the samples exceeds 105 MPa, and the porosity approximates to 15%. Further investigations require the production of samples in the form of a 6×6×30 mm bar in process conditions № 1 and № 2 (Figure 1).

All the samples produced in process conditions № 1 appear not to have any significant defects and meet the pre-set configuration (Figure 1, a). No visible defects are detected on the cubic sample produced in process conditions № 2, however, some defects occur on the lateral faces when synthesizing a bar (Figure 1, b). The defects are melted particles of powders, located on the lateral faces out of the scanning area. The defects originate mainly during the second phase of sintering the layer.

A 3D thermal model concentrated on sintering a single track and a single layer according to a pre-set strategy is developed to detect the causes of defects. The model problems are solved by a mathematical package COMSOL Multiphysics, which is an efficient interactive environment for FEM simulating and calculating a great number of scientific and technical issues based on differential



equations in partial derivatives (PDE). A lot of works are available, the authors of which deal with simulating the interaction between the laser beam and substances by means of this mathematical package [11-16].



Process conditions № 1: W=30 W; V=3000  
mm/min; S=0.1 mm; t=300 °C  
a)

Process conditions № 2: W=30 W; V=2000  
mm/min; S=0.1 mm; t=300 °C  
b)

**Figure 1.** SLM produced samples.

## 2. Methods of research

In the SLM process the powder is distributed, as a rule, over the whole operating area of the machine, and the section of sintering is far smaller (Figure 2)

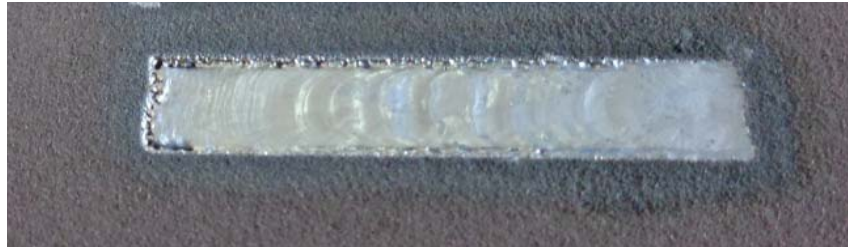


**Figure 2.** Sintering the rectangular samples of copper powder.

Therefore, for the purpose of modeling the geometry of powder in a freely poured condition can be limited by some millimeters relatively the section to be sintered.

In Figure 3 there is a model structure of sintering a single track on the powder layer. And in Figure 4 there is a model presented to sinter a single layer of powder poured on the previously sintered layers according to the pre-set strategy.

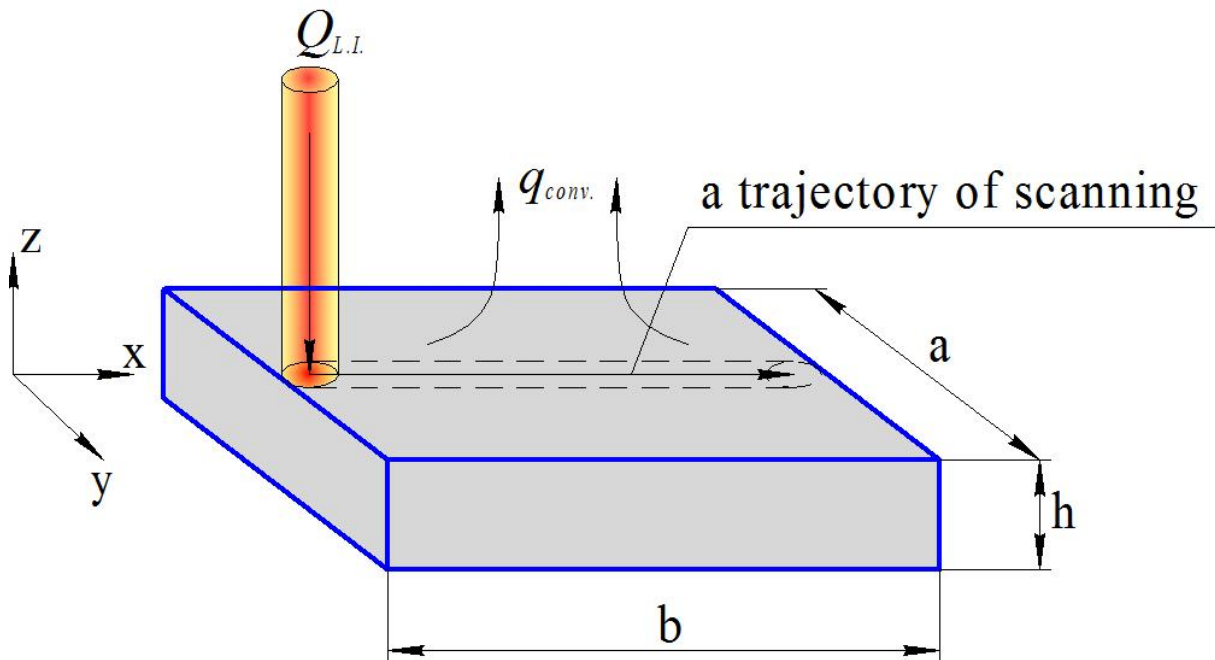


**Figure 3.** A model structure of single layer sintering.

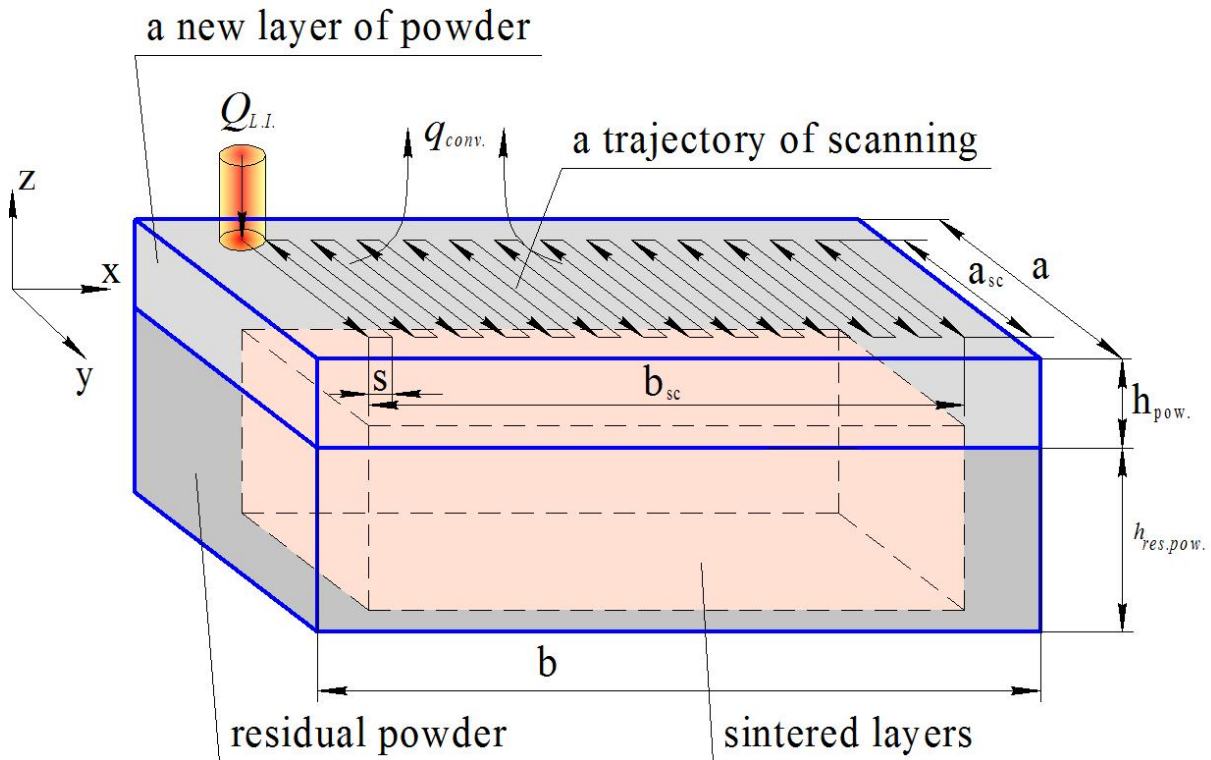


**Figure 4.** A model structure of sintering a single layer.

In the proposed model heat is distributed in the sample due to thermal conductivity only. A mathematical model describing the heat transfer by means of thermal conductivity is expressed by the thermal conductivity equation given below:

$$\rho C \frac{\partial T}{\partial t} - \nabla \cdot (k \nabla T) = Q, \quad (1)$$

where  $T$  – temperature;  $\rho$  – density;  $C$  – thermal capacity;  $k$  – thermal conductivity factor;  $Q$  – originating or absorbed heat.

Heat-transfer properties of powdered materials ( $\rho$ ,  $C$ ,  $k$ ) differ considerably from those of solid (monolithic) materials, they are identified experimentally and given in Table 1.

Laser impact is determined as a volumetric source of heat, the intensity of which depends on laser impact at various depths of the powder layer. The equation to calculate the laser impact heat is as follows:

$$Q(x, y, z) = Q_0(1 - R_C) \cdot \frac{A_C}{\pi \sigma_x \sigma_y} e^{-\left[ \frac{(x-x_0)^2}{2\sigma_x^2} + \frac{(y-y_0)^2}{2\sigma_y^2} \right]} \cdot e^{-A_C z}, \quad (2)$$

where  $Q_0$  – laser emission power;  $R_C$  – reflection coefficient;  $A_C$  – absorption coefficient;  $e^{-\left[ \frac{(x-x_0)^2}{2\sigma_x^2} + \frac{(y-y_0)^2}{2\sigma_y^2} \right]}$  – 2D Gauss distribution of emission power over the sample surface in the plane  $x, y$ ;  $e^{-A_C z}$  – exponential decay of power over the layer depth of a sample (Bouguer law).

The following assumptions are to be taken into consideration when implementing the model:

- reflection and absorption coefficients are constant;
- thermal effects of phase transformations are not taken into account;
- the surface of powder layer, along which the laser beam is moved, is parallel to the plane  $x-y$  of the system of coordinates;
- the upper plane of the powder layer is smoothed out according to  $z=0$ , consequently, the effect of power absorption can be expressed as follows:  $\exp(-A_C \cdot \text{abs}(z))$ ;
- the center of laser beam can be displaced via changing the variables  $x_0$  and  $y_0$ ;

- the diameter of laser beam is calculated on the base of standard deviation parameters  $\sigma_x$  and  $\sigma_y$ . Free convection with the upper surface of powder layer is taken into account as the boundary conditions. In Table 1 there are designations and values of variables provided, which we rely on when solving the problem.

**Table 1.** Designations and values of variables

A variable	Model for 1 track	Model for 1 layer
The laser spot radius relatively the coordinate axes $\sigma_x/\sigma_y$ , mm	0.1/0.1	0.1/0.1
Laser power $Q_0$ , W	15	30
Power distribution in the laser spot	Gauss distribution	Gauss distribution
Speed of scanning $v$ , mm/s	50	33.3
Scanning pitch $s$ , mm	-	0.1
Temperature of powder pre-heating, °C	25	400
Ambient temperature, °C	25	25
Dimensions of a new powder layer $a/b/h_{pow.}$ , mm	2.5/10/1	12/36/0.1
Dimensions of residual powder $a/b/h_{res.pow.}$ , mm	-	12/36/0.4
Scanning area dimensions $a_{sc}/b_{sc.}$ , mm	10	6/30
Dimensions of sintered layers $a_{sc}/b_{sc.}/h_{res.pow.}$	-	6/30/0.4
Thermal conductivity coefficient of powder, W/(m·°C)	0.36	0.36
Thermal capacity of the powder, J/(m <sup>3</sup> ·°C)	6.1	6.1

Heat-transfer properties of copper powder differ significantly from those of solid copper. The following properties of copper powder, necessary for modeling are identified experimentally: bulk density  $\rho_{pow.}=1.86 \text{ g/cm}^3$ , thermal conductivity coefficient  $k_{pow.}= 3.6 \times 10^{-3} \text{ W/(m} \cdot \text{°C)}$  and thermal capacity  $C_{pow.}=6.1 \text{ J/(m}^3 \cdot \text{°C)}$ .

The results of modeling single tracks are given in Figure 5.

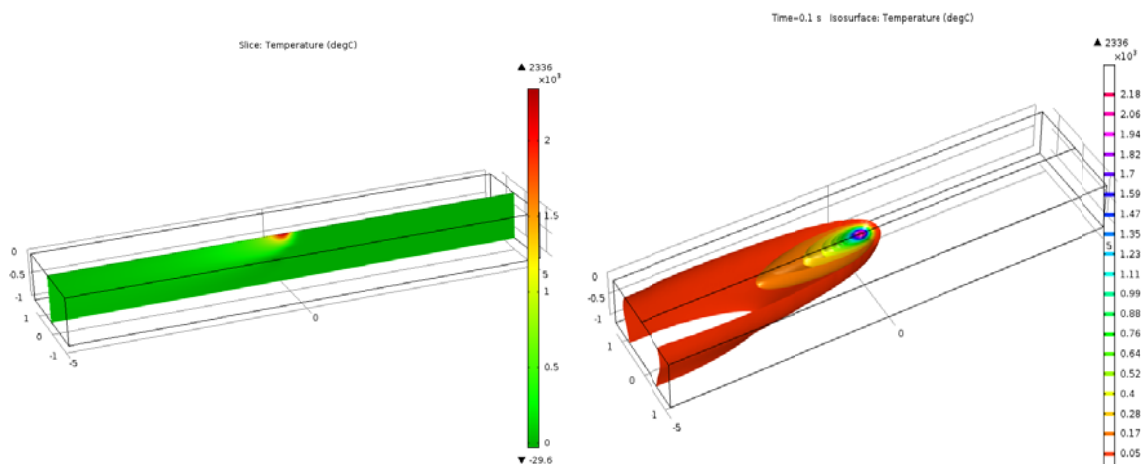


**Figure 5.** Temperature distribution when sintering 1 track.

The results of modeling a single track demonstrate that the depth of the zone with temperature above that of metal melting approximates to 0.2 mm. Therefore, the thickness of the sintered track is about 0.2 mm. These results meet the data of experiments outlined in [1] for powder PMS-1.

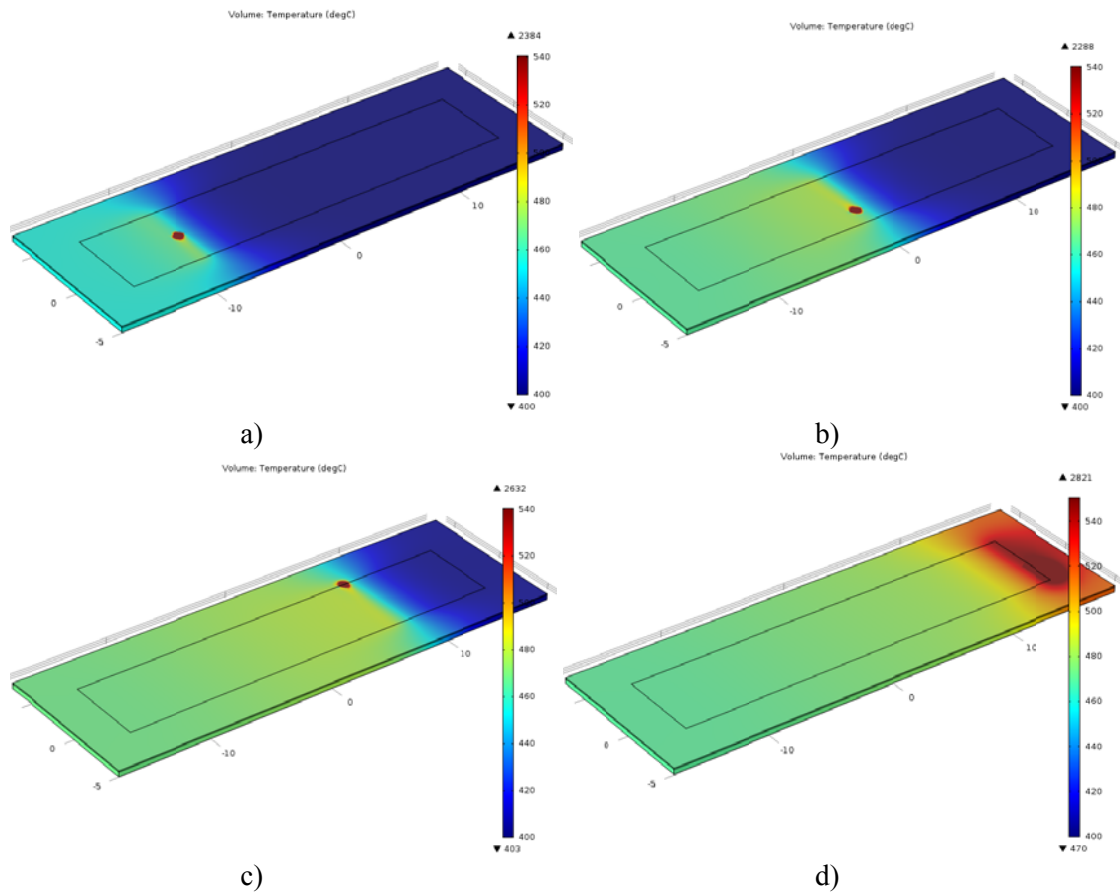


**Figure 6.** Temperature distribution when scanning a layer at various points of time: 10 s (a); 25 s (b); 40 s (c); 54 s (d).

When modeling the process of a single layer sintering, it is of interest how the temperature is distributed through the sample at various points of time. Since the temperature in the laser spot is much higher than that of a sample, temperature scaling is carried out for appropriate representation of temperature fields through the sample.

The results of modeling a single layer are given in Figure 6.

In Figure 8 one can see the plots of changing powder temperature 0.3 mm from the scanning area. The area under consideration is shown in Figure 7. Each plot demonstrates the distribution of temperature along the area to be studied with a 0.5 mm step at the points of time when a laser beam approaches the end line of the scanning area.

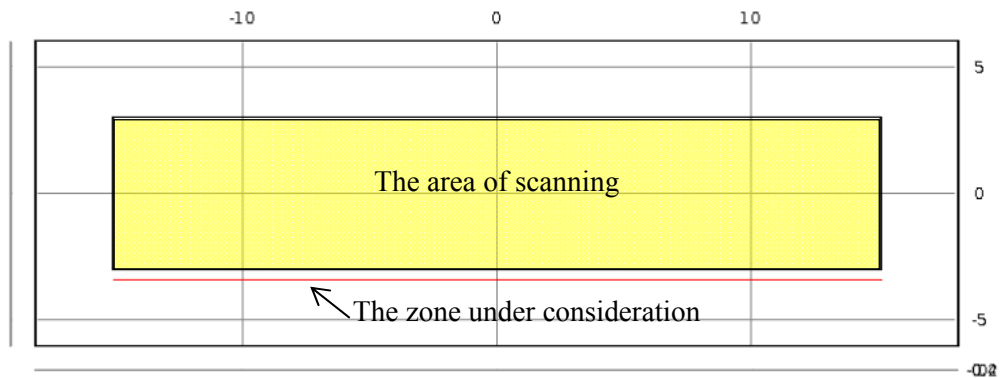


**Figure 7.** The zone to be examined along the area of scanning.



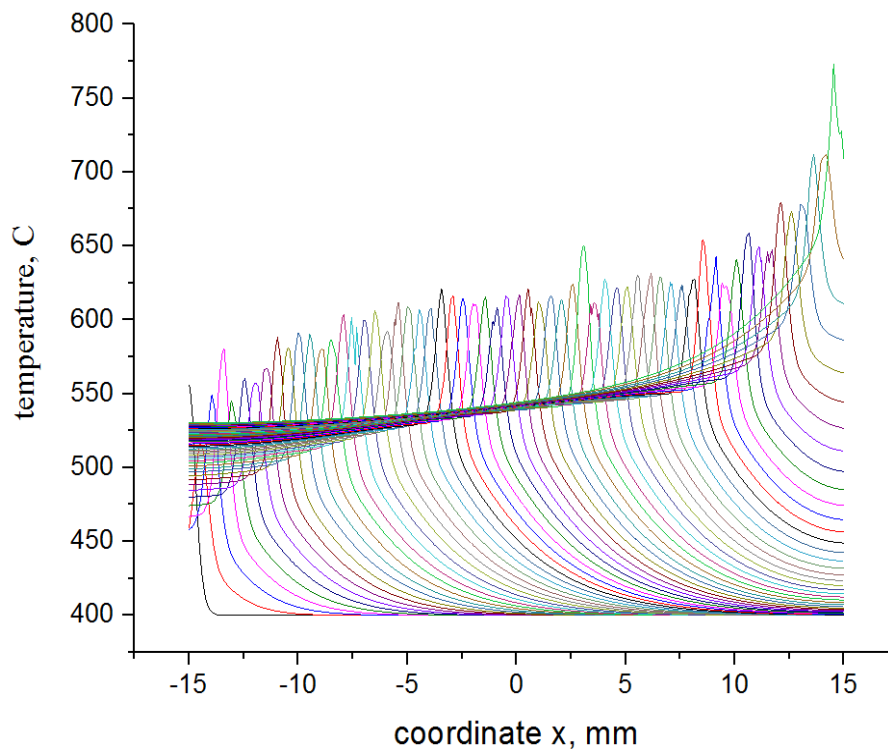


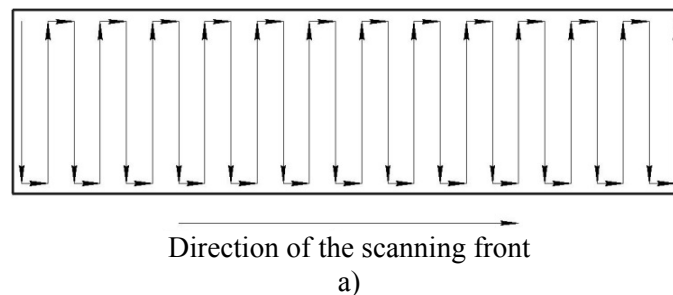
**Figure 8.** Powder temperature variation along the side line of the sintering area.

### 3. Results and discussion

Analyzing the data presented in Figure 6 and 8 one see that powder located on each side of a laser scanning area is heated when sintering a layer. The total time of scanning the surface is 54 seconds in the model. In the first 20 seconds the not-sintered powder is heated a little (Figure 6, a). In the period 20 to 40 seconds powder gets more heated, but then its temperature does not change much (Figure 6, b, c). During the end period 40 to 54 seconds the temperature of powder on the sides and in front of the scanning area goes up very fast (Figure 6, d).

During the second and third periods of heating the powder on the scanning area sides conditions are provided for self-melting of powder particles out of the scanning area under a slight energy impact (Figure 1, b). Non-uniform density distribution in the powder layer is also very important for self-melting of powder particles. This is possible because of different sizes and dendritic shape of powder particles when making a new layer of powder. These are the causes of non-uniform distribution of powder particles over the surface.

Decreasing the effect of powder heating on the sides is possible via changing the strategy of scanning (Figure 8).



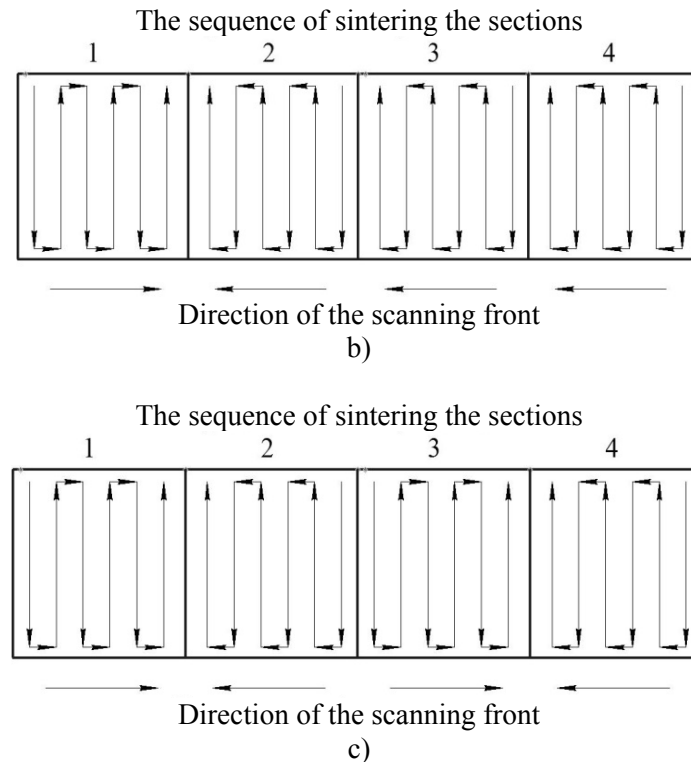


**Figure 9.** Strategies of scanning: a – complete line-oriented zigzag; b – “close to each other”; c – “away from each other”.

It is suggested to divide the area of scanning into sections and scan them “close to each other” (Figure 9, b) or “away from each other” (Figure 9, c). In these conditions the powder on the scanning area sides can get cooled down due to convection and thermal conductivity.

#### 4. Conclusion

The mathematical model describing the distribution of heat fields proposed in the paper makes it possible to determine the sections on the surface providing the most appropriate conditions for uncontrolled self-melting of powder particles. Alongside with key process variables of SLM synthesis one should consider the configuration of the layer to be scanned. It is proposed in this study to divide extended spaces of the surface into the sub-areas and scan them so that the free powder out of the scanning area get cooled down. This technological decision makes it possible to reduce the number of defect products.

#### References

- [1] Saprykin, A.A. Saprykin, N. A 2012. Engineering Support for Improving Quality of Layer-by-layer Laser Sintering *J. IFOST2012* **129–132**
- [2] Mani M., Lane B., Donmez A., Feng S., Fesperman R. Measurement Science Needs for Real-time Control of Additive Manufacturing Powder Bed Fusion Processes: Web: <http://dx.doi.org/10.6028/NIST.IR.8036>.
- [3] Saprykin A. A., Ibragimov E. A., Babakova E. V., Yakovlev V. I. 2015 Influence of mechanical activation of copper powder on physicomechanical changes in selective laser sintering products *J. AIP Conf. Proc.* **1683**, 020199
- [4] Saprykin A A, Gradoboyev A V, Yakovlev V I, Ibragimov E A, Babakova E V 2015 Comparative analysis of processes to activate copper powder PIMC-1 for SLS synthesizing products *J. Metal processing* **82–88** 3 (68)



- [5] Ibragimov E A, Saprykin A A, Babakova E V 2014 Influence of Laser Beam Machining Strategy at SLS Synthesis *J. Advanced Materials Research* **764–767** 1040
- [6] Saprykina N A, Saprykin A A, Borovikov I F, Sharkeev Y P, Influence of layer-by-layer laser sintering conditions on the quality of sintered surface layer of products 2015 *J. IOP Conf. Series: Materials Science and Engineering* **91** 012031.
- [7] Saprykina N A, Saprykin A A, Matrunchik M S, Formation of Surface Layer of Cobalt Chrome Molybdenum Powder Products with Differentiation of Laser Sintering Modes 2014 *J. Applied Mechanics and Materials* **294-298** 682
- [8] Galevsky G.V., Rudneva V.V., Garbuzova A.K., Valuev D.V., Titanium carbide: nanotechnology, properties, application 2015 *J. IOP Conference Series: Materials Science and Engineering*. **1-7** 91
- [9] Saprykin A. A., Babakova E. V., Ibragimov E. A. Fiber-Reinforced Composites in Rapid Prototyping Technologies 2015 *J. Applied Mechanics and Materials* **185-188** 770
- [10] Li C., Fu C.H., Guo Y.B., Fang F.Z. Fast Prediction and Validation of Part Distortion in Selective Laser Melting 2015 *J. Procedia Manufacturing*. Volume **1–11** 30.
- [11] Thijs L Kempen K, Kruth J-P ,Van Humbeeck J Fine- structured aluminium products with controllable texture by Selective Laser Melting of pre-alloyed AlSi10Mg powder 2013 *J. Acta Materialia* **1809-1819** 61
- [12] Tomashchuk I., Jouvard J.-M., Sallamand P., Numerical modeling of copper-steel laser joining 2007 Excerpt from the Proceedings of the COMSOL Users Conference 2007 Grenoble [electronic resource] access mode: [www.researchgate.net/publication/266443725\\_Numerical\\_modeling\\_of\\_copper-steel\\_laser\\_joining](http://www.researchgate.net/publication/266443725_Numerical_modeling_of_copper-steel_laser_joining).
- [13] Biancol N., Manca O., Nardini S. Tamburrino S. Transient Heat Conduction in Semi-Infinite Solids Irradiated by a Moving Heat Source 2007 Excerpt from the Proceedings of the COMSOL Users Conference Grenoble [electronic resource] access mode: [www.researchgate.net/publication/234006400\\_Transient\\_Heat\\_Conduction\\_in\\_Solids\\_Irradiated\\_by\\_a\\_Moving\\_Heat\\_Source](http://www.researchgate.net/publication/234006400_Transient_Heat_Conduction_in_Solids_Irradiated_by_a_Moving_Heat_Source)
- [14] Karbasi H. COMSOL Assisted Simulation of Laser Engraving / Excerpt from the Proceedings of the COMSOL Conference 2010 Boston [electronic resource] access mode: <http://www.comsol.com/paper/comsol-assisted-simulation-of-laser-engraving-7574>
- [15] V. Bruyere, C. Touvre, P.Namy, Comparison between Phase Field and ALE Methods to model the Keyhole Digging during Spot Laser Welding / Excerpt from the Proceedings of the COMSOL Conference 2013Rotterdam [electronic resource] access mode: [www.comsol.com/paper/download/181647/bruyere\\_paper.pdf](http://www.comsol.com/paper/download/181647/bruyere_paper.pdf)
- [16] M. Darif, N. Semmar, Numerical Simulation of Si Nanosecond Laser Annealing by COMSOL Multiphysics / Excerpt from the Proceedings of the COMSOL Conference 2008 Hannover [electronic resource] access mode: <http://www.comsol.com/paper/numerical-simulation-of-si-nanosecond-laser-annealing-by-comsol-multiphysics-5586>
- [17] Pryor, Roger W. Multiphysics modeling using COMSOL : a first principles approach / Roger W. Pryor. 2010.
- [18] Kumar S, Kruth J-P 2009 Composites by Rapid Prototyping Technology *J. Materials & Design* **1–23**.
- [19] Murali K, Chatterjee A N, Saha P, Palai R, Kumar S, Roy S K, Mishra P K, Choudhury A R 2003 Direct selective laser sintering of iron-graphite powder mixture *J. Journal of Materials Processing Technology* **179–185** 136